

Heat transport through a two-level system under continuous quantum measurement

Tsuyoshi Yamamoto,^{1,*} Yasuhiro Tokura,¹ and Takeo Kato²

¹*Faculty of Pure and Applied Sciences, University of Tsukuba, Tsukuba, Ibaraki 305-8571, Japan*

²*Institute for Solid State Physics, the University of Tokyo, Kashiwa, Chiba 277-8581, Japan*

(Dated: August 19, 2022)

We study the backaction of quantum measurements on heat transport through a two-level system by considering the continuous projective measurement onto an eigen state of the two-level system. For the non-selective measurement, the backaction appears as a dephasing effect on the two-level system. We formulate the heat current under the selective measurement with a stochastic master equation and show that the cross-correlation between the measurement outcomes and the heat current contains information on the backaction. We expect that our findings can be verified by using a platform of superconducting circuits.

Introduction.— Measurement is indispensable to access the information on a system. Quantum measurements usually disturb a quantum system and thus destroy quantum correlations, in striking contrast to the classical realm in which unperturbed measurement is possible in principle [1]. This backaction of the quantum measurement triggers many intriguing phenomena. For example, in quantum many-body systems constituting large-scale entanglements, the quantum backaction induces various nontrivial effects, e.g., measurement-induced phase transitions [2–6], non-Hermitian dynamics [7–9], and suppression of the Kondo effect [10]. Moreover, quantum backaction has been observed in well-controllable systems of cold atoms [11–15] and of solid-state nanostructures [16]. In particular, a superconducting circuit is an ideal platform for exploring quantum backaction on many-body states. This is because experimental efforts toward the realization of quantum computers have enabled high-speed readout of qubits' information and controlled interaction of a single qubit with other qubits or electromagnetic fields [17, 18].

Continuous measurement has a significant impact on transport through a small quantum object since transport properties reflect quantum states of such an object [19, 20]. The simplest example is heat transport through a two-level system, i.e., a qubit. Recent developments in experimental techniques have enabled us to accurately measure heat current through a qubit and have stimulated theoretical and experimental studies [21–27]. Contrary to its apparent simplicity, quantum transport via a qubit exhibits many-body effects due to strong qubit-bath coupling, e.g., the Kondo effect [28–34] and quantum phase transitions [28, 29, 35–42]. Moreover, since the transferred heat is related to entropy production [27, 43], heat transport under measurement is also a key to demonstrating Maxwell's demon and shedding light on the relation between energy and information [44–49]. In that sense, it is cross-cutting to consider measurement effects in heat transport from the viewpoint of uniting condensed matter physics and information theory.

In this Letter, we consider heat transport through a

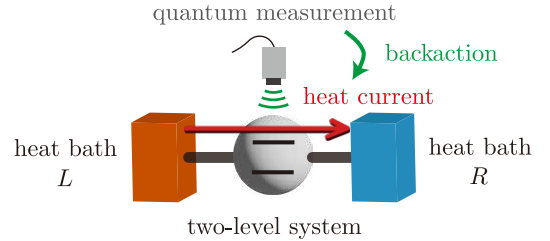


FIG. 1. Schematic diagram of the model considered in this Letter. A two-level system is coupled to two bosonic heat baths and an apparatus for continuous quantum measurement. When the temperature of the heat bath L is higher than that of the heat bath R , the heat current flows from the heat bath L to R through the two-level system. The quantum measurement of the two-level system affects the heat current, which is called *backaction*.

two-level system and examine how heat transport is affected by a continuous projective measurement onto an eigenstate of the two-level system (see Fig. 1). We calculate the heat current by using the master equation which takes quantum measurement processes followed by post-selection into account. First, we show that the dephasing induced by continuous measurement modifies the heat current. To clarify the backaction in detail, we further calculate the cross-correlation between the heat current and the measurement outcomes in the selective measurement scheme. We expect that the present experimental techniques enable the measurement setup to be realized in the form of superconducting circuits.

Model.— We consider heat current between two heat baths through a two-level system under continuous quantum measurement (see Fig. 1). The system is described by the spin-boson model, whose Hamiltonian consists of three terms as $H = H_{\text{TLS}} + H_{\text{B}} + H_{\text{I}}$. The two-level system is described by $H_{\text{TLS}} = -(\hbar\Delta/2)\sigma_x$, where Δ (> 0) is the tunneling amplitude and σ_i ($i = x, y, z$) are the Pauli matrices. The heat baths are modeled by collections of harmonic oscillators as

$$H_{\text{B}} = \sum_r H_{\text{B},r} = \sum_{rk} \hbar\omega_{rk} b_{rk} b_{rk}^\dagger, \quad (1)$$

where b_{rk} (b_{rk}^\dagger) is a bosonic annihilation (creation) operator of the k th mode in the heat bath r ($= L, R$) with energy $\hbar\omega_{rk}$. The interaction between the two-level system and the heat baths is described by

$$H_I = \sum_r H_{I,r} = -\frac{\sigma_z}{2} \sum_{rk} \hbar\lambda_{rk} (b_{rk} + b_{rk}^\dagger), \quad (2)$$

with coupling strength λ_{rk} . The properties of the heat baths are determined by the spectral density $I_r(\omega) \equiv \sum_k \lambda_{rk}^2 \delta(\omega - \omega_{rk})$. In this Letter, we focus on an Ohmic heat bath whose spectral density is written in the form $I_r(\omega) = 2\alpha_r \omega e^{-\omega/\omega_c}$, where α_r is a dimensionless coupling strength and ω_c is a cutoff frequency.

We consider the backaction induced by a quantum measurement onto the ground state $|+\rangle$ (or onto the excited state $|-\rangle$) of the two-level system, where $|\pm\rangle$ are eigenstates of σ_x ($\sigma_x |\pm\rangle = \pm |\pm\rangle$). We define projection operators, $P_\pm = |\pm\rangle\langle\pm| = (I \pm \sigma_x)/2$, and operators for the corresponding continuous quantum measurements, $M_\pm = \sqrt{\gamma_m^\pm} P_\pm$, where γ_m^\pm indicates the strength of the measurement.

Non-selective measurement.— First, let us consider a non-selective quantum measurement in which the measured values do not affect the subsequent dynamics. In this case, the quantum dynamics can be described by the Lindblad equation after taking the ensemble average over the measurement outcomes [50]:

$$\frac{d\rho}{dt} = -\frac{i}{\hbar} [H, \rho] + \mathcal{D}_m[\rho], \quad (3)$$

where $\mathcal{D}_m[\rho] = \sum_{i=\pm} (M_i \rho M_i^\dagger - \{M_i^\dagger M_i, \rho\}/2)$. Here, ρ denotes the density matrix and $[\cdot, \cdot]$ and $\{\cdot, \cdot\}$ are the commutator and anti-commutator, respectively. Assuming that the system-bath coupling is weak ($\alpha_r \ll 1$), the Lindblad equation for the reduced density matrix, $\tilde{\rho} = \text{tr}_B[\rho]$, is obtained as [51]

$$\frac{d\tilde{\rho}}{dt} = -\frac{i}{\hbar} [H_{\text{TLS}}, \tilde{\rho}] + \mathcal{D}_B[\tilde{\rho}] + \mathcal{D}_m[\tilde{\rho}], \quad (4)$$

where $\mathcal{D}_B[\tilde{\rho}] = \sum_{r,i=\pm} \Gamma_{ri} (\sigma^i \tilde{\rho} \sigma^{-i} - \{\sigma^{-i} \sigma^i, \tilde{\rho}\}/2)$, $\sigma^\pm = (\sigma_z \pm i\sigma_y)/2$, $\Gamma_{r+} = (\pi/2)n_r(\Delta)I_r(\Delta)$ and $\Gamma_{r-} = (\pi/2)[n_r(\Delta) + 1]I_r(\Delta)$ are the absorption and emission rates, respectively, and $n_r(\omega) = (e^{\beta_r \hbar\omega} - 1)^{-1}$ is the Bose-Einstein distribution function at temperature $T_r = 1/(k_B \beta_r)$ of the heat bath r . In the Lindblad equation (4), the effect of the measurement is described by $\mathcal{D}_m[\tilde{\rho}] = \gamma_m(\sigma_x \tilde{\rho} \sigma_x - \tilde{\rho})/4$ with $\gamma_m = \gamma_m^+ + \gamma_m^-$. This indicates that the backaction of the non-selective measurement appears through dephasing, whose amplitude is given by $\gamma_p = \gamma_m/2$ [52]. Note that we cannot get the information on which state is detected in this scheme.

Heat current under the non-selective measurement.— The heat current flowing from the heat bath L to R through the two-level system is defined as $J_L = -dH_{B,L}/dt$. Assuming that the temperature difference

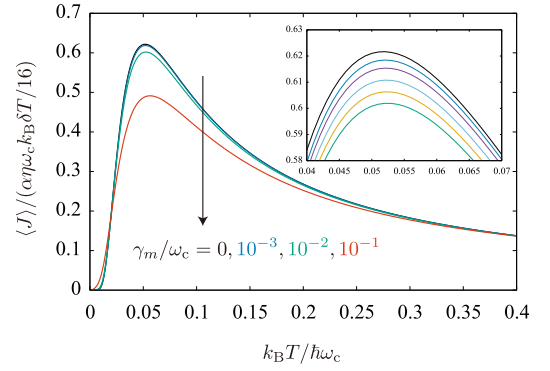


FIG. 2. Temperature dependence of the steady-state heat current under a non-selective projective quantum measurement for $\Delta/\omega_c = 0.1$, $\alpha = 0.01$, $\varepsilon/\omega_c = 0$ and $\gamma_m/\omega_c = 0, 10^{-3}, 10^{-2},$ and 10^{-1} . The inset is an enlarged view near the peaks calculated for $\gamma_m/\omega_c \times 10^3 = 0, 1, 2.5, 5, 7.5,$ and 10 from top to bottom.

between the two heat baths is sufficiently small, i.e., $T_{L/R} = T \pm \delta T/2$ with $\delta T/T \ll 1$, we can obtain an analytical formula for the steady-state heat current $\langle J \rangle = \langle J_L \rangle = -\langle J_R \rangle$ up to first order in δT by using the Keldysh formalism, as [33, 53, 54]

$$\langle J \rangle = \frac{\alpha \eta k_B \delta T}{16} \int_0^\infty d\omega S(\omega) \tilde{I}(\omega) \frac{(\beta \hbar \omega)^2}{\sinh(\beta \hbar \omega)}, \quad (5)$$

where $\alpha = \alpha_L + \alpha_R$, $\eta = 4\alpha_L \alpha_R / \alpha^2$, $\tilde{I}(\omega) = I_r(\omega)/\alpha_r$, and $\beta = 1/(k_B T)$. Here, $S(\omega)$ is the Fourier transformation of a symmetrized correlation function, $S(t) = \langle \{\sigma_z(t), \sigma_z(0)\} \rangle / 2$. From the Lindblad equation (4), $S(\omega)$ reads [55]

$$S(\omega) = \frac{4\tilde{\Gamma}_s(\Delta^2 + \tilde{\Gamma}_s^2)}{[(\omega - \Delta)^2 + \tilde{\Gamma}_s^2][(\omega + \Delta)^2 + \tilde{\Gamma}_s^2]}, \quad (6)$$

where $\tilde{\Gamma}_s = (\Gamma_s + \gamma_m)/2$ and $\Gamma_s = \sum_r (\Gamma_{r+} + \Gamma_{r-})$ [56].

The steady-state heat current $\langle J \rangle$ is plotted as a function of temperature in Fig. 2. As the strength of continuous quantum measurement, γ_m , increases, the peak of the heat current is suppressed. As indicated, this suppression is induced by an increase in the level broadening in the response function (6) ($\Gamma_s \rightarrow 2\tilde{\Gamma}_s$) due to the additional damping induced by the non-selective quantum measurement.

Selective measurement.— Next, let us discuss selective projective measurement onto $|\pm\rangle$ by considering physical quantities which depend on measurement outcomes. For this purpose, we treat discontinuous changes in the density matrix, i.e., quantum jumps using the stochastic master equation for a conditional density matrix ρ_c [1, 57]:

$$\rho'_c = \rho_c - \frac{i}{\hbar} [H, \rho_c] \Delta t + \mathcal{D}_m^{(1)}[\rho_c] \Delta t + \mathcal{D}_m^{(2)}[\rho_c] \Delta N_i, \quad (7)$$

where $\rho'_c = \rho_c(t + \Delta t)$, $\mathcal{D}_m^{(1)}[\rho_c] = -\{M_i^\dagger M_i, \rho_c\}/2 + \text{tr}[\rho_c M_i^\dagger M_i] \rho_c$, $\mathcal{D}_m^{(2)}[\rho_c] = M_i \rho_c M_i^\dagger / \text{tr}[\rho_c M_i^\dagger M_i] - \rho_c$, and we have neglected the higher-order terms of $\Delta t \Delta N \sim o(\Delta t)$. The total density matrix is reproduced by taking the ensemble average, $\rho = E[\rho_c]$, where $E[\cdot]$ denotes the ensemble average. The measurement outcomes are described by a Poisson process with a stochastic variable ΔN_i , which takes 1 when the two-level system is detected as being in state $|i\rangle$ and 0 otherwise during time Δt . The ensemble average of the Poisson variable is written as $E[\Delta N_i] = \text{tr}[\rho_c M_i^\dagger M_i] \Delta t = \gamma_m^i (1 \pm \langle \sigma_x \rangle_c) \Delta t / 2$.

For the weak system-bath coupling ($\alpha_r \ll 1$), the time-evolution equation for the reduced density matrix $\tilde{\rho}_c = \text{tr}_B[\rho_c]$ is obtained in the same manner as the non-selective case, as

$$\begin{aligned} \tilde{\rho}'_c &= \tilde{\rho}_c - \frac{i}{\hbar} [H_{\text{TLS}}, \tilde{\rho}_c] \Delta t + \mathcal{D}_B[\tilde{\rho}_c] \Delta t \\ &+ \mathcal{D}_m^{(1)}[\tilde{\rho}_c] \Delta t + \mathcal{D}_m^{(2)}[\tilde{\rho}_c] \Delta N_i. \end{aligned} \quad (8)$$

From this equation, one can derive time-evolution equations for the conditional coherences and population $\langle \sigma_i(t) \rangle_c$ [58].

Heat current under the selective measurement.— The heat current under the condition that the state $|i\rangle$ of the two-level system is not detected ($\Delta N_i = 0$) is formulated as follows [59]. In the Markov limit and assuming that the coherence can be neglected on the relevant time scale, the heat current flowing from the heat bath r ($= L, R$) into the two-level system is expressed as [60] $\langle J_r(t) \rangle_c = \hbar \Delta [\Gamma_{r+} p_c^g(t) - \Gamma_{r-} p_c^e(t)]$, where $p_c^{g(e)} = \langle g(e) | \tilde{\rho}_c | g(e) \rangle = (1 \pm \langle \sigma_x \rangle_c) / 2$ is the population of the ground (excited) state. For simplicity, we will consider a symmetric heat bath ($\alpha/2 = \alpha_L = \alpha_R$) hereafter. When the temperature difference δT is sufficiently small, the net heat current flowing from the heat bath L to R , $\langle J(t) \rangle = (\langle J_L(t) \rangle - \langle J_R(t) \rangle) / 2$, can be expressed to first order in δT as

$$\langle J(t) \rangle_c = \frac{\pi I(\Delta) k_B \delta T}{8 \text{sinhc}^2(\beta \hbar \Delta / 2)} \langle \sigma_x(t) \rangle_c, \quad (9)$$

where $I(\Delta) = \sum_r I_r(\Delta)$ and $\text{sinhc}(x) = \sinh(x)/x$.

A sample of the conditional heat current $\langle J(t) \rangle_c$ under a projective measurement onto $|+\rangle$ is shown in Fig. 3. Several quantum jumps in the time evolution of $\langle J(t) \rangle_c$ are characteristic to the selective measurement. After detection, the conditional heat current jumps to a definite value because the state of the two-level system is projected to the state $|+\rangle$. On the contrary, the heat current tends to relax to a stationary point during periods in which there were no detections ($\Delta N_+ = 0$). Thus, the dynamics of the conditional heat current can be described by stochastic quantum trajectories composed of continuous dynamics during the no-detection periods ($\Delta N_+ = 0$) and quantum jumps ($\Delta N_+ = 1$). The conditional heat current under selective measurement onto

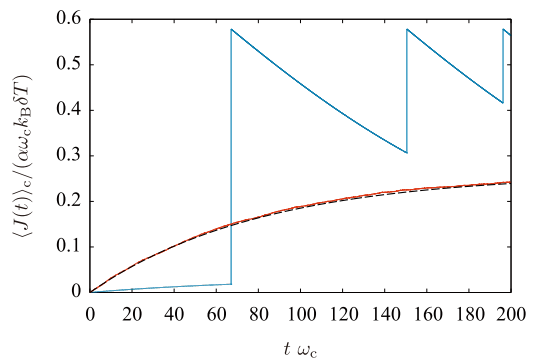


FIG. 3. Heat current under projective quantum measurement onto $|+\rangle$ as a function of time. The parameters are $\Delta/\omega_c = 0.1$, $\alpha = 0.01$, $\gamma_m^+/\omega_c = 0.01$, and $k_B T/\hbar \omega_c = 0.1$. The blue line represents the heat current obtained from one sample of quantum trajectories which includes three quantum jumps in the range of the plot. The numerical ensemble average of the heat current, $E[\langle J(t) \rangle_c]$, using 10^4 quantum trajectories (the red line) coincides with the heat current obtained under the non-selective measurement (the black dashed line). We set the initial conditions as $\langle \sigma_x(0) \rangle_c = \langle \sigma_y(0) \rangle_c = 0$ and $\langle \sigma_z(0) \rangle_c = 1$.

$|-\rangle$ can be formulated in a similar way. The ensemble average of the conditional heat current on these trajectories, $E[\langle J(t) \rangle_c]$, (the red line in Fig. 3) reproduces the heat current under the non-selective measurement, $\langle J(t) \rangle = \pi I(\Delta) (\beta \hbar \Delta)^2 / [16 \text{sinhc}(\beta \hbar \Delta)] (1 - e^{-\Gamma_s t}) k_B \delta T$ (the dashed line in Fig. 3) [61].

Cross-correlation.— To observe the backaction induced by the continuous quantum measurement onto $|i = \pm\rangle$, let us consider the cross-correlation between the heat current and the measurement outcomes defined by

$$F_i(t) = E \left[\frac{1}{t_1 - t_0} \int_{t_0}^{t_1} dt' \delta \Delta N_i(t') \delta \langle J(t+t') \rangle_c \right], \quad (10)$$

where $\delta A = A - E[A]$. For the sake of convenience, we will define the normalized cross-correlation as $\mathcal{F}_\pm(t) = F_\pm(t) / \{\pi I(\Delta) k_B \delta T / [16 \text{sinhc}^2(\beta \hbar \Delta / 2)]\}$ (see also Eq. (9)). We can obtain the following analytic form for $t = \Delta t$:

$$\frac{\mathcal{F}_\pm(\Delta t)}{\Delta t} = \pm \frac{\gamma_m^\pm}{t_1 - t_0} \int_{t_0}^{t_1} dt' [1 - \langle \sigma_x(t') \rangle_c^2], \quad (11)$$

where we have used $E[\Delta N_\pm(t') \langle \sigma_x(t' + \Delta t) \rangle_c] = \pm E[\Delta N_\pm(t')]$ and noting that $\langle \sigma_x \rangle_c = 1$ just after detection ($\Delta N_i = 1$). At $t_0, t_1 \gg \Gamma_s^{-1}$, we can neglect the effect of the upper and lower limits in the integral by plugging the stationary solution, $\langle \sigma_x \rangle_{\text{ss}} = \tanh(\beta \hbar \Delta / 2)$ [62], into $\langle \sigma_x(t') \rangle_c$ in the integral. Then, we obtain the cross-correlation, in the limit of $\Delta t \rightarrow 0^+$, as $F_\pm(0^+)/\Delta t = \pm \gamma_m^\pm \pi I(\Delta) k_B \delta T / [16 \text{sinhc}^2(\beta \hbar \Delta)]$. This expression indicates that the cross-correlations under the projective measurement onto $|\pm\rangle$ have opposite signs, i.e., $F_+(0^+)/\gamma_m^+ = -F_-(0^+)/\gamma_m^- > 0$.

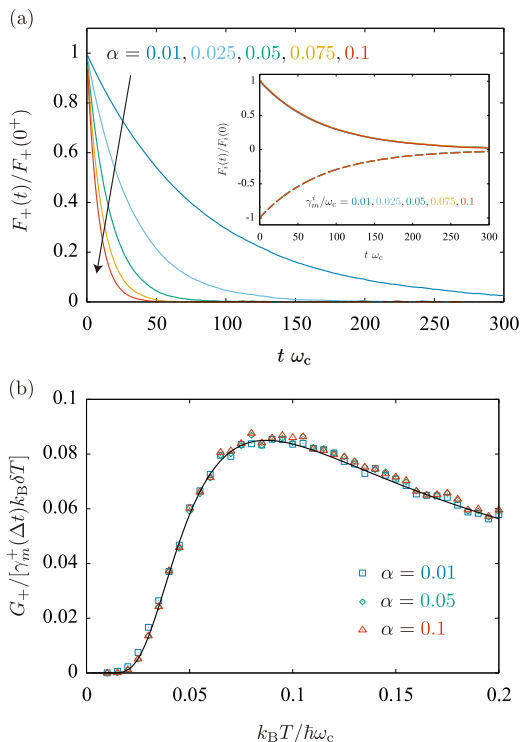


FIG. 4. (a) Cross-correlation function $F_+(t)$ under selective projective measurement onto $|+\rangle$ for different values of $\alpha = 0.01, 0.025, 0.05, 0.075, 0.1$ using 10^4 ensembles. The parameters are $\Delta/\omega_c = 0.1$, $\gamma_m^+ = 0.01$, $k_B T/\hbar\omega_c = 0.1$, $t_0\omega_c = 500$, and $t_1\omega_c = 1000$. The inset shows the cross-correlation functions, $F_+(t)$ (solid lines) and $F_-(t)$ (dashed lines), for different $\gamma_m^i = 0.01, 0.025, 0.05, 0.075, 0.1$. (b) Integrated cross-correlation G_+ as a function of temperature for $\alpha = 0.01, 0.05, 0.1$ using 5×10^3 ensembles. The other parameters are the same as in panel (a). The solid line represents an analytic form $\gamma_m^+ (\Delta t) k_B \delta T \tanh(\beta\hbar\Delta/2)/[2 \sinh c(\beta\hbar\Delta)]^2$, which is obtained from the numerical fitting for $F_+(t)$ in panel (a). For both panels, the initial conditions are the same as those in Fig. 3.

Figure 4 (a) shows the results of numerical simulations of the cross-correlation $F_+(t)$. The cross-correlation decays exponentially, $F_+(t)/F_+(0^+) = e^{-\Gamma t}$ with a decay rate Γ that depends on the coupling strength α ; the cross-correlation decays more quickly as the system-bath coupling is stronger. From the numerical fitting, we found that the decay rate is linear to α and in good agreement with the symmetric rate Γ_s . As shown in the inset of Fig. 4 (a), the normalized cross-correlations $F_i(t)/F_i(0^+)$ for different $\gamma_m^i = 0.01 - 0.1$ collapse to the same curve. This indicates that the strength of the quantum measurement appears only in the amplitude of the cross-correlation, being linear to γ_m^i . The inset also indicates that $F_+(t)/\gamma_m^+ = -F_-(t)/\gamma_m^- > 0$ holds for an arbitrary time.

Finally, let us consider the integrated cross-correlation,

$G_i = \int_0^\infty dt F_i(t)$. The temperature dependence of the integrated cross-correlation is shown in Fig. 4 (b) for $\alpha = 0.01, 0.05, 0.1$. The numerical simulations for different values of α collapse to the same curve, which indicates that the integrated cross-correlation is independent of α . The integrated cross-correlation $G_i/\Delta t$ coincides with the analytic form $\pm \gamma_m^i k_B \delta T \tanh(\beta\hbar\Delta/2)/[8 \sinh^2(\beta\hbar\Delta)]$ indicated by the solid line in Fig. 4 (b).

Experimental realization.— We expect that our theoretical proposal can be verified experimentally by using a platform consisting of superconducting circuits. The heat current through a cavity-qubit system can be measured with present technology, as demonstrated in a recent experiment [24]. In this experiment, a transmon-type qubit was used as a two-level system with frequency $\Delta \approx 5.30$ GHz, corresponding to $\hbar\Delta/k_B \approx 40.5$ mK, and the measurement was performed in the temperature range of $T \approx 75 \sim 350$ mK. Thus, the condition, $\hbar\Delta \approx k_B T$, required to observe the backaction discussed in this Letter can be fulfilled. To measure the integrated cross-correlation, the outcomes from continuous monitoring of the two-level system should be used as a trigger for the subsequent measurement of the integrated heat current within a finite period, which should be larger than the inverse of the decay rate Γ_s^{-1} . This conditional heat current will deviate from the steady-state heat current without monitoring. We emphasize that the sign of this deviation depends on which of the states $|\pm\rangle$ is used for the continuous quantum measurement on the two-level system.

Summary.— We considered heat transport through a two-level system under a continuous projective measurement onto the ground or excited state of the two-level system. We found, in the non-selective measurement scheme, that the heat current is affected by the quantum measurement through the dephasing effect. In addition, to observe the backaction effect directly, we calculated the cross-correlation between the measurement outcomes and the heat current. We found that the cross-correlation depends on which of the eigenstates of the two-level system is to be measured and that the integrated cross-correlation is enhanced when the temperature becomes comparable with the energy splitting of the two-level system. Our work, focusing on a weak system-bath coupling, represents a starting point for further research on measurement-induced transport phenomena. It remains challenging to clarify new quantum many-body effects induced by quantum measurement.

Y.T. and T.K. acknowledge JSPS KAKENHI for Grants (Nos. JP20K03831 and JP20H01827). Y.T. and T.Y. were supported by JST Moonshot R&D-MILLENNIA Program (Grant Number JPMJMS2061).

-
- * yamamoto.tsuyoshi.ga@u.tsukuba.ac.jp
- [1] H. M. Wiseman and G. J. Milburn, *Quantum Measurement and Control* (Cambridge University Press, Cambridge, 2009).
- [2] Y. Li, X. Chen, and M. P. A. Fisher, Phys. Rev. B **98**, 205136 (2018).
- [3] Y. Li, X. Chen, and M. P. A. Fisher, Phys. Rev. B **100**, 134306 (2019).
- [4] B. Skinner, J. Ruhman, and A. Nahum, Phys. Rev. X **9**, 031009 (2019).
- [5] M. Ippoliti, M. J. Gullans, S. Gopalakrishnan, D. A. Huse, and V. Khemani, Phys. Rev. X **11**, 011030 (2021).
- [6] T. Minato, K. Sugimoto, T. Kuwahara, and K. Saito, Phys. Rev. Lett. **128**, 010603 (2022).
- [7] T. E. Lee and C.-K. Chan, Phys. Rev. X **4**, 041001 (2014).
- [8] Y. Ashida, S. Furukawa, and M. Ueda, Phys. Rev. A **94**, 053615 (2016).
- [9] Y. Ashida and M. Ueda, Phys. Rev. Lett. **120**, 185301 (2018).
- [10] M. Hasegawa, M. Nakagawa, and K. Saito, arXiv:2111.07771 (2022).
- [11] K. W. Murch, K. L. Moore, S. Gupta, and D. M. Stamper-Kurn, Nature Physics **4**, 561 (2008).
- [12] N. Syassen, D. M. Bauer, M. Lettner, T. Volz, D. Dietze, J. J. García-Ripoll, J. I. Cirac, G. Rempe, and S. Dürr, Science **320**, 1329 (2008).
- [13] B. Zhu, B. Gadway, M. Foss-Feig, J. Schachenmayer, M. L. Wall, K. R. A. Hazzard, B. Yan, S. A. Moses, J. P. Covey, D. S. Jin, J. Ye, M. Holland, and A. M. Rey, Phys. Rev. Lett. **112**, 070404 (2014).
- [14] Y. S. Patil, S. Chakram, and M. Vengalattore, Phys. Rev. Lett. **115**, 140402 (2015).
- [15] T. Tomita, S. Nakajima, I. Danshita, Y. Takasu, and Y. Takahashi, Science Advances **3**, 1701513 (2017).
- [16] D. Bischoff, M. Eich, O. Zilberberg, C. Rössler, T. Ihn, and K. Ensslin, Nano Lett. **15**, 6003 (2015).
- [17] M. Hatridge, S. Shankar, M. Mirrahimi, F. Schackert, K. Geerlings, T. Brecht, K. M. Sliwa, B. Abdo, L. Frunzio, S. M. Girvin, R. J. Schoelkopf, and M. H. Devoret, Science **339**, 178 (2013).
- [18] J. P. Groen, D. Ristè, L. Tornberg, J. Cramer, P. C. de Groot, T. Picot, G. Johansson, and L. DiCarlo, Phys. Rev. Lett. **111**, 090506 (2013).
- [19] J. Z. Bernád, M. Jääskeläinen, and U. Zülicke, Phys. Rev. B **81**, 073403 (2010).
- [20] J. Rech and S. Kehrein, Phys. Rev. Lett. **106**, 136808 (2011).
- [21] M. Meschke, W. Guichard, and J. P. Pekola, Nature **444**, 187 (2006).
- [22] A. V. Timofeev, M. Helle, M. Meschke, M. Möttönen, and J. P. Pekola, Phys. Rev. Lett. **102**, 200801 (2009).
- [23] M. Partanen, K. Y. Tan, J. Govenius, R. E. Lake, M. K. Mäkelä, T. Tanttu, and M. Möttönen, Nature Physics **12**, 460 (2016).
- [24] A. Ronzani, B. Karimi, J. Senior, Y.-C. Chang, J. T. Peltonen, C. Chen, and J. P. Pekola, Nat. Phys. **14**, 991 (2018).
- [25] J. Senior, A. Gubaydullin, B. Karimi, J. T. Peltonen, J. Ankerhold, and J. P. Pekola, Communications Physics **3**, 40 (2020).
- [26] O. Maillet, D. Subero, J. T. Peltonen, D. S. Golubev, and J. P. Pekola, Nature Communications **11**, 4326 (2020).
- [27] J. P. Pekola and B. Karimi, Rev. Mod. Phys. **93**, 041001 (2021).
- [28] A. J. Leggett, S. Chakravarty, A. T. Dorsey, M. P. A. Fisher, A. Garg, and W. Zwerger, Rev. Mod. Phys. **59**, 1 (1987).
- [29] U. Weiss, *Quantum Dissipative Systems*. (World Scientific, Singapore, 2012).
- [30] A. Hewson, *The Kondo Problem to Heavy Fermions* (Cambridge University Press, New York, 1993).
- [31] F. Guinea, V. Hakim, and A. Muramatsu, Phys. Rev. B **32**, 4410 (1985).
- [32] K. Le Hur, Phys. Rev. B **85**, 140506(R) (2012).
- [33] K. Saito and T. Kato, Phys. Rev. Lett. **111**, 214301 (2013).
- [34] T. Yamamoto, M. Kato, T. Kato, and K. Saito, New J. Phys. **20**, 093014 (2018).
- [35] P. W. Anderson and G. Yuval, J. Phys. C: Solid State Phys. **4**, 607 (1971).
- [36] J. M. Kosterlitz, Phys. Rev. Lett. **37**, 1577 (1976).
- [37] G. De Filippis, A. de Candia, G. Di Bello, C. A. Perroni, L. M. Cangemi, A. Nocera, M. Sassetti, R. Fazio, and V. Cataudella, arXiv:2205.11555 (2022).
- [38] S. K. Kehrein, A. Mielke, and P. Neu, Z. Phys. B Condensed Matter **99**, 269 (1995).
- [39] S. K. Kehrein and A. Mielke, Phys. Lett. A **219**, 313 (1996).
- [40] R. Bulla, N.-H. Tong, and M. Vojta, Phys. Rev. Lett. **91**, 170601 (2003).
- [41] A. Winter, H. Rieger, M. Vojta, and R. Bulla, Phys. Rev. Lett. **102**, 030601 (2009).
- [42] T. Yamamoto and T. Kato, Phys. Rev. B **98**, 245412 (2018).
- [43] J. P. Pekola, Nature Physics **11**, 118 (2015).
- [44] L. Szilard, Z. Phys. **53**, 840 (1929).
- [45] H. S. Leff and A. F. Rex, eds., *Maxwell's Demon 2: Entropy, Classical and Quantum Information, Computing* (IOP Publishing, Bristol, 2003).
- [46] T. Sagawa and M. Ueda, Phys. Rev. Lett. **100**, 080403 (2008).
- [47] T. Sagawa and M. Ueda, Phys. Rev. Lett. **104**, 090602 (2010).
- [48] J. V. Koski, V. F. Maisi, J. P. Pekola, and D. V. Averin, PNAS **111**, 13786 (2014).
- [49] J. V. Koski, V. F. Maisi, T. Sagawa, and J. P. Pekola, Phys. Rev. Lett. **113**, 030601 (2014).
- [50] H. Carmichael, *An Open System Approach to Quantum Optics* (Springer, Berlin, 1993).
- [51] H. Breuer and F. Petruccione, *The Theory of Open Quantum Systems* (Oxford University Press, New York, 2007).
- [52] E. Iyoda, T. Kato, T. Aoki, K. Edamatsu, and K. Koshino, J. Phys. Soc. Jpn. **82**, 014301 (2013).
- [53] T. Ojanen and A.-P. Jauho, Phys. Rev. Lett. **100**, 155902 (2008).
- [54] K. Saito, Europhys. Lett. **83**, 50006 (2008).
- [55] Using the quantum regression theorem [51], the dynamics of the correlation function $C_{zz}(t) = \langle \sigma_z(t) \sigma_z(0) \rangle$ are determined by the differential equation, $\ddot{C}_{zz} + 2\tilde{\Gamma}_s \dot{C}_{zz} + (\Delta^2 + \tilde{\Gamma}_s^2) C_{zz} = 0$, and its solution is given by $C_{zz}(t) = e^{-\tilde{\Gamma}_s t} [\cos(\Delta t) + (\tilde{\Gamma}_s / \Delta) \sin(\Delta t)]$ under the initial conditions $C_{zz}(0) = 1$ and $\dot{C}_{zz}(0) = 0$.
- [56] The heat transport process discussed in this letter is

called a sequential tunneling process, which can describe heat transport for $k_B T \sim \hbar \Delta$. However, at lower temperatures, $k_B T \lesssim 0.1 \hbar \Delta$, the sequential tunneling process is suppressed, and thus the co-tunneling process becomes dominant, in which the higher-order interaction between the two-level system and the heat baths plays the important role [34, 63].

- [57] H. M. Wiseman and G. J. Milburn, Phys. Rev. A **47**, 1652 (1993).
- [58] See Supplemental Material for details on the numerical calculation of the conditional coherences and population.
- [59] In our simulation, the heat current under the condition, $\Delta N_i = 1$, can be defined arbitrarily, because the number of time steps in this condition is much less than the number in $\Delta N_i = 0$ in the limit $\Delta t \rightarrow 0$. See Supplemental Material for details.
- [60] D. Segal and A. Nitzan, J. Chem. Phys. **122**, 194704 (2005).
- [61] We can reproduce this expression for the heat current at $t \rightarrow \infty$ by plugging $S(\omega) \approx \pi \delta(\omega - \Delta)$ into Eq. (5).
- [62] The stationary solution of $\langle \sigma_x \rangle$ is calculated by solving the differential equations $\langle \dot{\sigma}_x \rangle = -\Gamma_s \langle \sigma_x \rangle - \Gamma_a$ under the steady-state condition $\langle \dot{\sigma}_x \rangle = 0$.
- [63] T. Ruokola and T. Ojanen, Phys. Rev. B **83**, 045417 (2011).

Supplemental Materials for:

“Heat transport through a two-level system under continuous quantum measurement”

I. NUMERICAL CALCULATION OF CONDITIONAL COHERENCES AND POPULATION

Here, we provide details on the numerical calculation of the conditional coherences and population $\langle \sigma_i(t) \rangle_c$, which allowed us to plot Fig. 3 in the main text.

We start by expressing the reduced conditional density matrix using the Bloch vector as

$$\tilde{\rho}_c(t) = \frac{1}{2} (I + \langle \vec{\sigma}(t) \rangle_c \cdot \vec{\sigma}) = \frac{1}{2} \begin{pmatrix} 1 + \langle \sigma_z(t) \rangle_c & \langle \sigma_x(t) \rangle_c - i \langle \sigma_y(t) \rangle_c \\ \langle \sigma_x(t) \rangle_c + i \langle \sigma_y(t) \rangle_c & 1 - \langle \sigma_z(t) \rangle_c \end{pmatrix}. \quad (\text{S1})$$

The stochastic master equation (8) then reads, in the matrix representation,

$$\begin{aligned} & \begin{pmatrix} 1 + \langle \sigma_z(t + \Delta t) \rangle_c & \langle \sigma_x(t + \Delta t) \rangle_c - i \langle \sigma_y(t + \Delta t) \rangle_c \\ \langle \sigma_x(t + \Delta t) \rangle_c + i \langle \sigma_y(t + \Delta t) \rangle_c & 1 - \langle \sigma_z(t + \Delta t) \rangle_c \end{pmatrix} \\ &= \begin{pmatrix} 1 + \langle \sigma_z(t) \rangle_c & \langle \sigma_x(t) \rangle_c - i \langle \sigma_y(t) \rangle_c \\ \langle \sigma_x(t) \rangle_c + i \langle \sigma_y(t) \rangle_c & 1 - \langle \sigma_z(t) \rangle_c \end{pmatrix} - \Delta \begin{pmatrix} \langle \sigma_y(t) \rangle_c & i \langle \sigma_z(t) \rangle_c \\ -i \langle \sigma_z(t) \rangle_c & - \langle \sigma_y(t) \rangle_c \end{pmatrix} \Delta t \\ & - \frac{\Gamma_s}{2} \begin{pmatrix} \langle \sigma_z(t) \rangle_c & 2 \langle \sigma_x(t) \rangle_c - i \langle \sigma_y(t) \rangle_c \\ 2 \langle \sigma_x(t) \rangle_c + i \langle \sigma_y(t) \rangle_c & - \langle \sigma_z(t) \rangle_c \end{pmatrix} \Delta t - \Gamma_a \begin{pmatrix} 0 & 1 \\ 1 & 0 \end{pmatrix} \Delta t \\ & \mp \frac{\gamma_m^\pm}{2} \begin{pmatrix} \langle \sigma_x(t) \rangle_c & 1 \\ 1 & \langle \sigma_x(t) \rangle_c \end{pmatrix} \Delta t \mp \frac{\gamma_m^\pm}{2} \langle \sigma_x(t) \rangle_c \begin{pmatrix} 1 + \langle \sigma_z(t) \rangle_c & \langle \sigma_x(t) \rangle_c - i \langle \sigma_y(t) \rangle_c \\ \langle \sigma_x(t) \rangle_c + i \langle \sigma_y(t) \rangle_c & 1 - \langle \sigma_z(t) \rangle_c \end{pmatrix} \Delta t \\ & - \begin{pmatrix} \langle \sigma_z(t) \rangle_c & \langle \sigma_x(t) \rangle_c \mp 1 - i \langle \sigma_y(t) \rangle_c \\ \langle \sigma_x(t) \rangle_c \mp 1 + i \langle \sigma_y(t) \rangle_c & - \langle \sigma_z(t) \rangle_c \end{pmatrix} \Delta N_\pm, \end{aligned} \quad (\text{S2})$$

where $\Gamma_a = \sum_r (\Gamma_{r+} - \Gamma_{r-}) = -\sum_r \pi \alpha_r \Delta e^{-\Delta/\omega_c}$. Here, \pm denotes the projective measurement onto an eigen state $|\pm\rangle$ of σ_x . Therefore, the time evolution of the conditional coherences and population can be described by

$$\langle \sigma_x(t + \Delta) \rangle_c = \langle \sigma_x(t) \rangle_c - \left[\Gamma_s \langle \sigma_x(t) \rangle_c \pm \frac{\gamma_m^\pm}{2} (1 - \langle \sigma_x(t) \rangle_c^2) + \Gamma_a \right] \Delta t - (\langle \sigma_x(t) \rangle_c \mp 1) \Delta N_\pm, \quad (\text{S3})$$

$$\langle \sigma_y(t + \Delta t) \rangle_c = \langle \sigma_y(t) \rangle_c + \left(\Delta \langle \sigma_z(t) \rangle_c - \frac{\Gamma_s}{2} \langle \sigma_y(t) \rangle_c \pm \frac{\gamma_m^\pm}{2} \langle \sigma_x(t) \rangle_c \langle \sigma_y(t) \rangle_c \right) \Delta t - \langle \sigma_y(t) \rangle_c \Delta N_\pm, \quad (\text{S4})$$

$$\langle \sigma_z(t + \Delta t) \rangle_c = \langle \sigma_z(t) \rangle_c - \left(\Delta \langle \sigma_y(t) \rangle_c + \frac{\Gamma_s}{2} \langle \sigma_z(t) \rangle_c \mp \frac{\gamma_m^\pm}{2} \langle \sigma_x(t) \rangle_c \langle \sigma_z(t) \rangle_c \right) \Delta t - \langle \sigma_z(t) \rangle_c \Delta N_\pm. \quad (\text{S5})$$

Next, the Poisson variable ΔN_\pm , which takes 0 or 1, is generated with the probability,

$$P[\Delta N_\pm = 1] = \frac{\gamma_m^\pm \Delta t}{2} (1 \pm \langle \sigma_x(t) \rangle_c), \quad P[\Delta N_\pm = 0] = 1 - P[\Delta N_\pm = 1]. \quad (\text{S6})$$

Then, we can obtain $\langle \sigma_i(t + \Delta t) \rangle_c$ numerically by using values of $\langle \sigma_i(t) \rangle_c$ and Eqs. (S3)-(S5) iteratively from the initial conditions, $\langle \sigma_x(0) \rangle_c = \langle \sigma_y(0) \rangle_c = 0$ and $\langle \sigma_z(0) \rangle_c = 1$.

II. HEAT CURRENT UNDER THE SELECTIVE MEASUREMENT FOR $\Delta N_i = 1$

Here, we discuss the heat current when the detected state of the two-level system is an eigen state $|i = +\rangle$ or $|i = -\rangle$ ($\Delta N_i = 1$).

Using the definition of the heat current and the Heisenberg equation, the heat current is expressed as

$$\langle J_L(t) \rangle_c = - \left\langle \frac{dH_{B,L}}{dt} \right\rangle_c = \frac{i}{2} \sum_k \lambda_{Lk} \hbar \omega_{Lk} \left\langle \sigma_z(t) \left[b_{Lk}(t) - b_{Lk}^\dagger(t) \right] \right\rangle_c. \quad (\text{S7})$$

where $\langle \mathcal{O} \rangle_c = \text{tr}[\rho_c \mathcal{O}]$. Instantaneously after the detection at t , the conditional density matrix is projected to the eigen state $|i\rangle$,

$$\rho_c(t) = \frac{P_i \rho_c(t - \Delta t) P_i}{\langle P_i(t) \rangle_c}. \quad (\text{S8})$$

where $P_\pm = |\pm\rangle \langle \pm|$ is the projective operator. By plugging the conditional density matrix (S8) into the bracket in the heat current (S7), we obtain

$$\left\langle \sigma_z(t) \left[b_{Lk}(t) - b_{Lk}^\dagger(t) \right] \right\rangle_c = \text{tr} \left[\rho_c(t) \sigma_z \left(b_{Lk} - b_{Lk}^\dagger \right) \right] = \frac{\text{tr} \left[\rho_c(t - \Delta t) P_i \sigma_z P_i \left(b_{Lk} - b_{Lk}^\dagger \right) \right]}{\langle P_i(t) \rangle_c} = 0, \quad (\text{S9})$$

where we have used the cyclic property, $[P_i, b_{Lk}^\dagger] = 0$, and $P_i \sigma_z P_i = 0$. Therefore, when $\Delta N_i = 1$, heat current does not flow, i.e., $\langle J_L(t) \rangle_c = 0$.

Finally, we note that the contribution of the heat current at the detection does not matter for the ensemble values in our numerical simulations at the $\Delta t \rightarrow 0$ limit.
